Proton air cross section measurements with air shower experiments

Gian Carlo Trinchero
INAF-IFSI
Torino

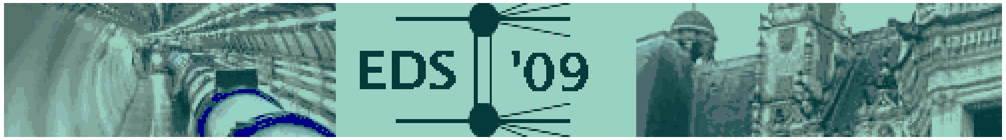

EDS'09: 13° International Conference on Elastic & Diffractive Scattering, 2 July 2009

Outline

- Introduction
- *p*-air inelastic cross section measurements
  - Frequency Attenuation method: Constant Ne-Nμ cuts
  - X_{max} distribution
- Experimental results
  - Systematic Uncertainties of measurement
  - Heavier primaries contribution
- *p*-air inelastic cross section results
- *pp* cross section
- Conclusions

Motivations

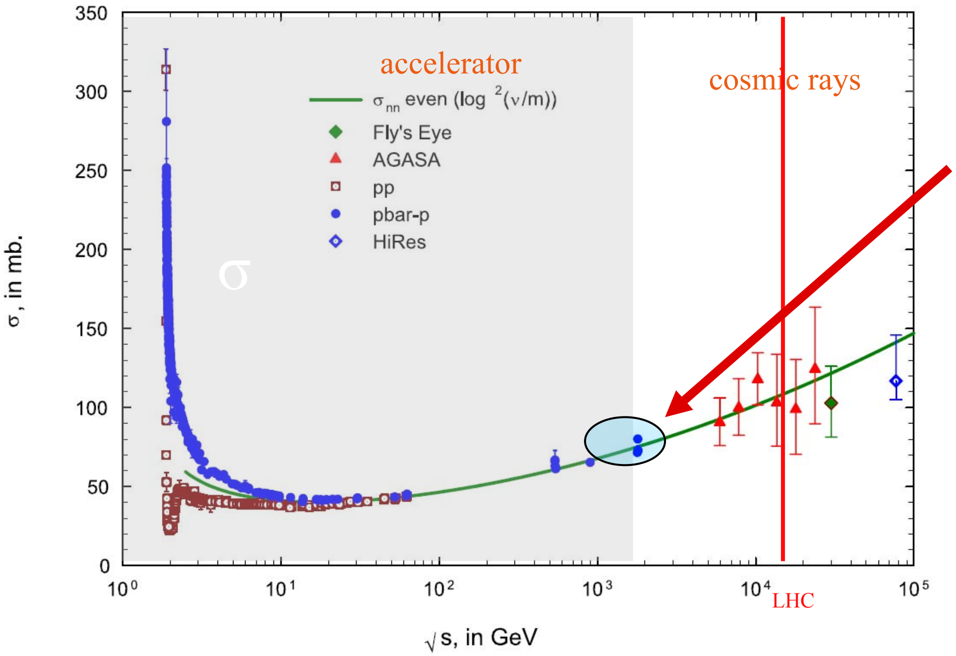

Accelerator data up to $\sqrt{s}$=1.8 TeV
Available results differ of ≈10% exceeding the statistical uncertainties of the individual measurements

- PLB 243 (1990),158
- PRD 50 (1994),5550

Motivations

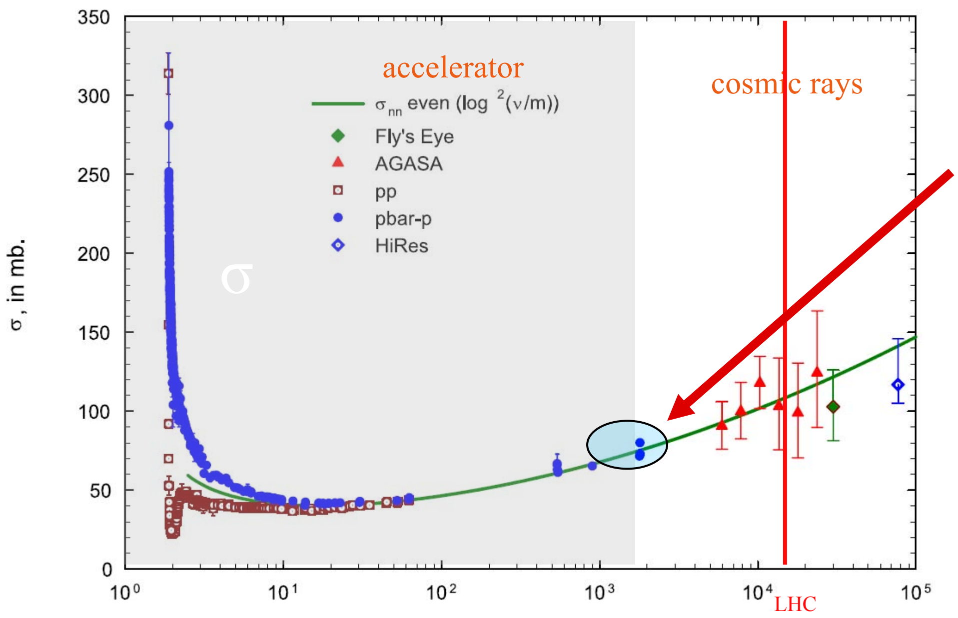

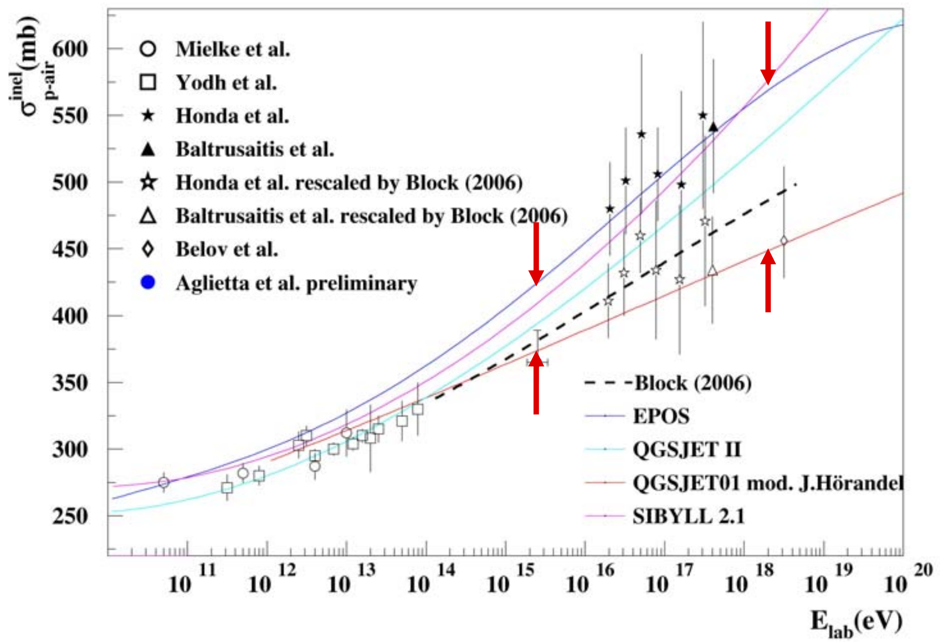

Accelerator data up to $\sqrt{s}$=1.8 TeV
Available results differ of ≈10% exceeding the statistical uncertainties of the individual measurements

- PLB 243 (1990),158
- PRD 50 (1994),5550

The interpretation of EAS measurements rely on simulation based on Hadronic Interaction Models which exhibit large differences at the highest energies

Motivations

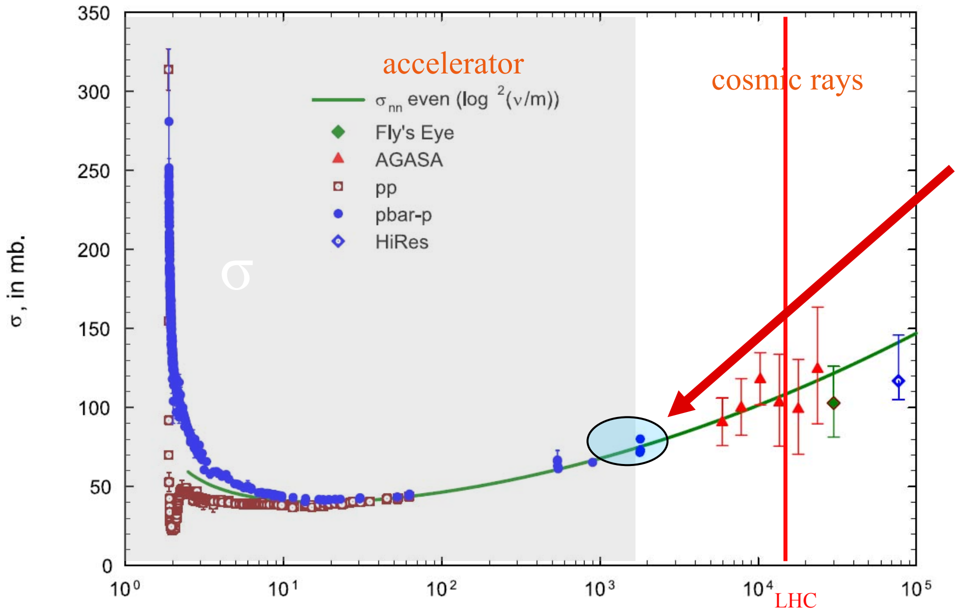

Accelerator data up to √s=1.8 TeV
Available results differ of ≈10% exceeding the statistical uncertainties of the individual measurements

- PLB 243 (1990),158
- PRD 50 (1994),5550

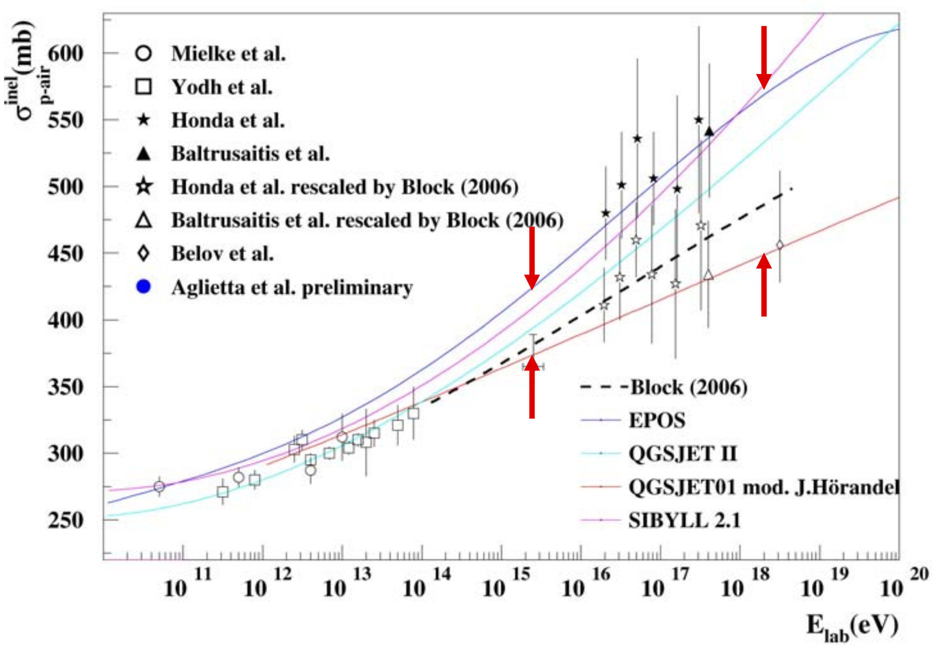

The interpretation of EAS measurements rely on simulation based on Hadronic Interaction Models which exhibit large differences at the highest energies

$\sigma^{in}_{p\text{-}air}$ and σ^{tot}_{pp} are related (Glauber)
Result of different calculations differing ≈20% around √s=2 TeV

EAS Longitudinal Development

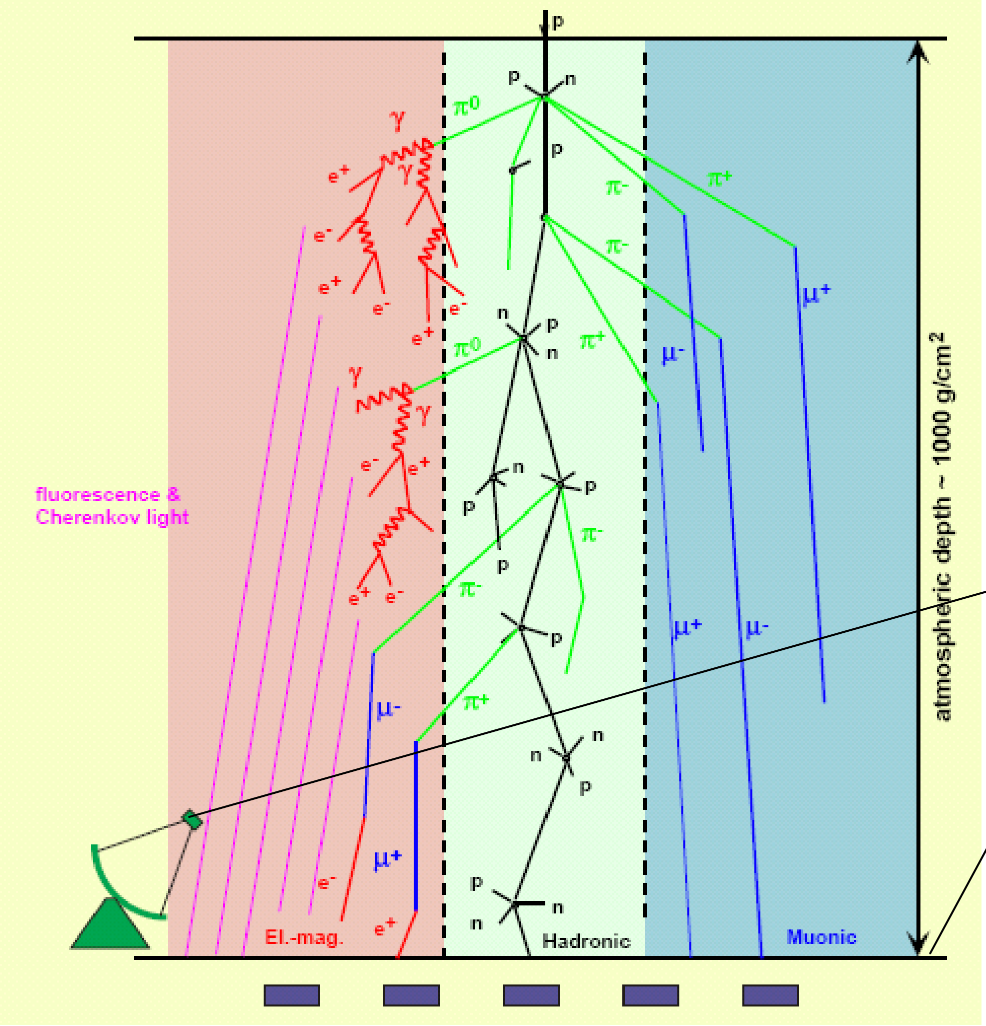

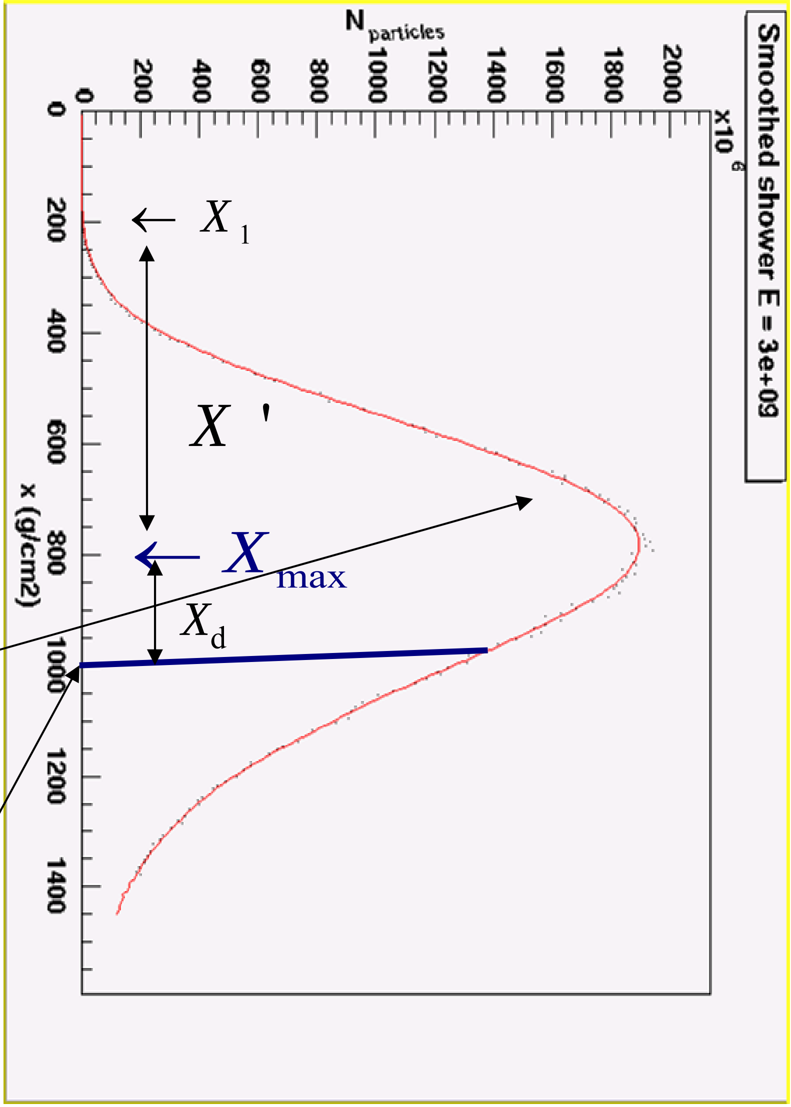

X_{max} Distribution

Fly's Eye PRL 52 (1984) 1380

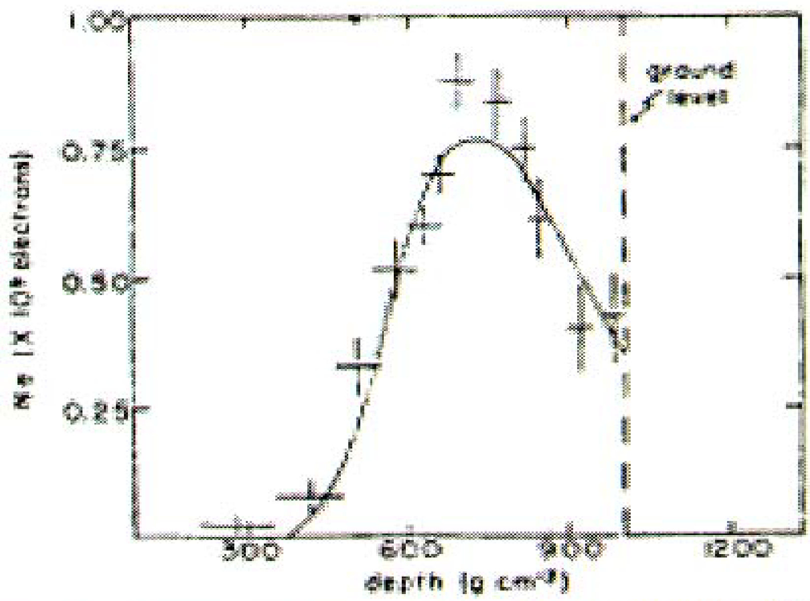

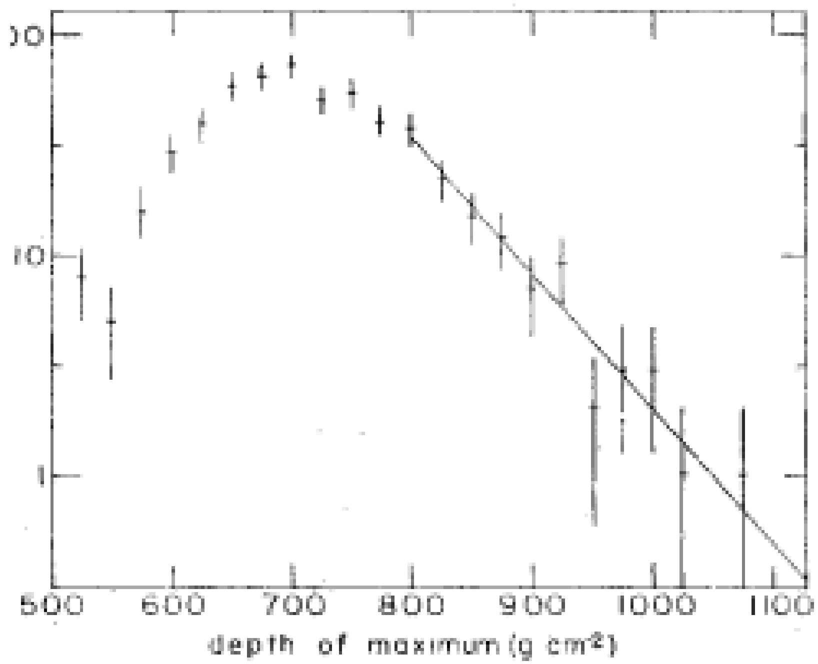

Fig. 1 An extensive air shower that survives all data cuts. The curve is a GaisserHillas shower-development function: shower parameters E=1.3 EeV and X_{max} =727 ± 33 g cm^{-2} give the best fit.

Frequency Attenuation: Constant N_e-N_μ cuts

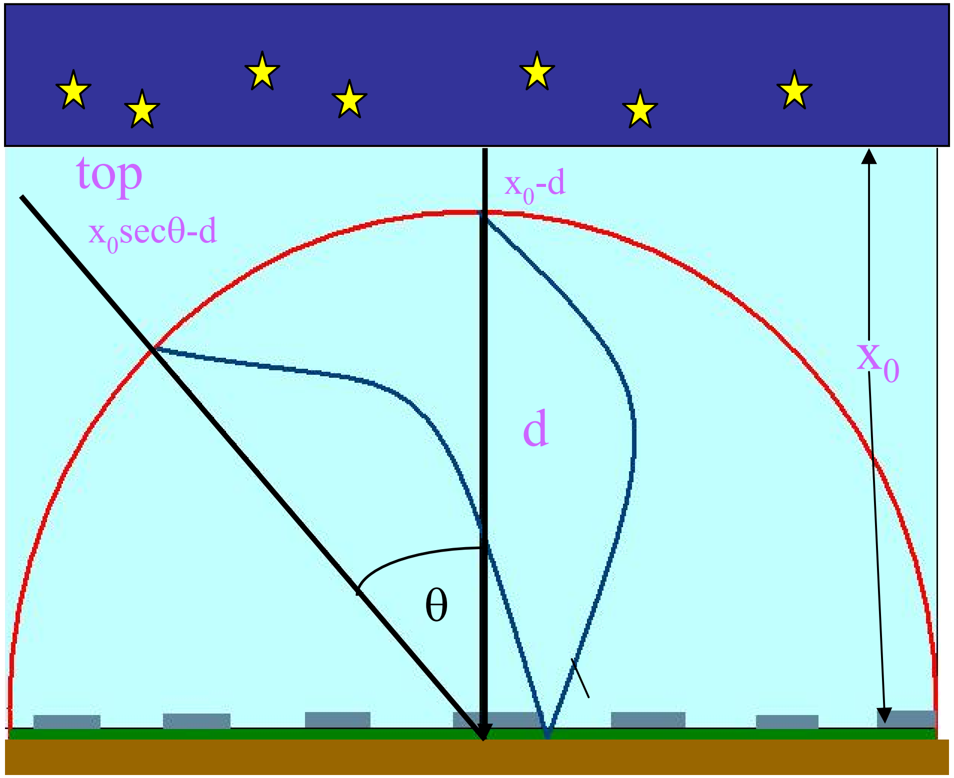

Primary Energy E_0 selected by using muon number

$E_1 < E_0 < E_2 \Rightarrow N_{\mu,1} < N_\mu < N_{\mu,2}$

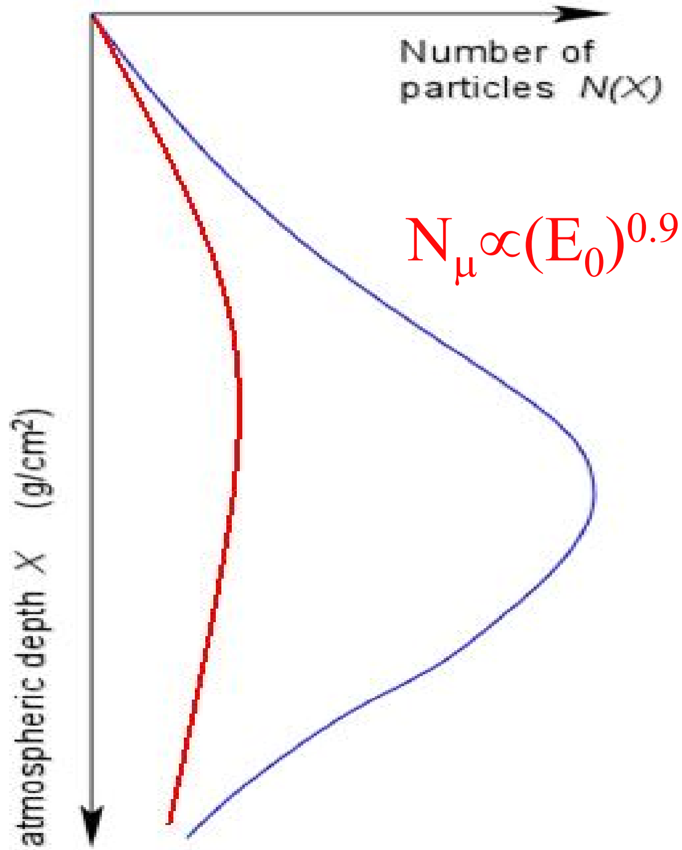

Frequency Attenuation: Constant N_e-N_μ cuts

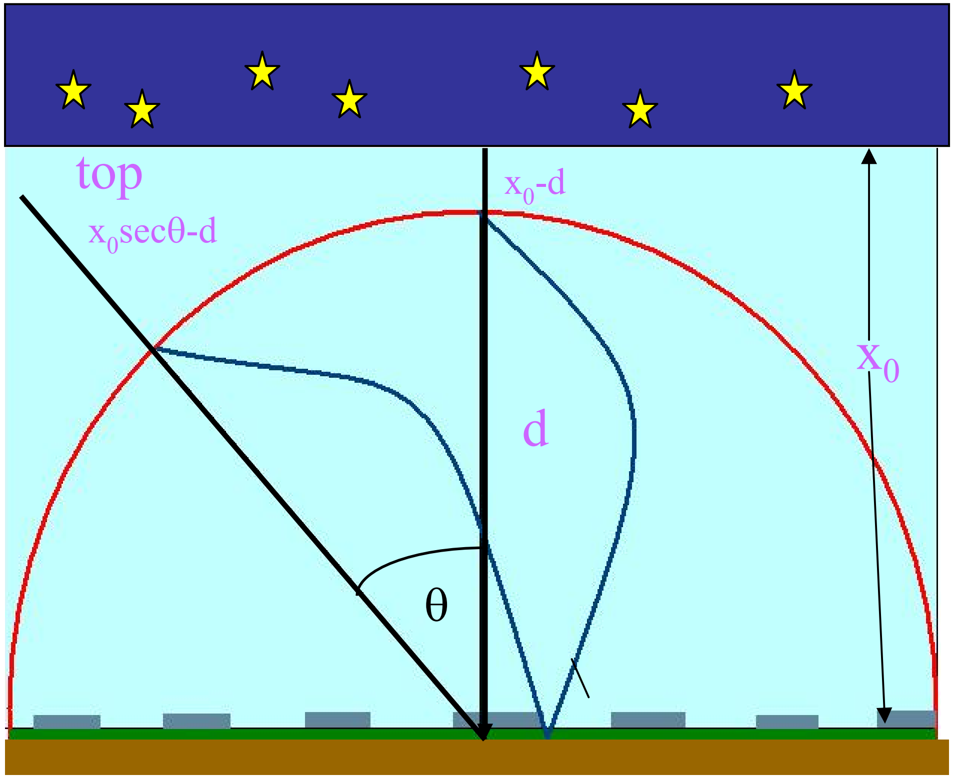

Primary Energy E_0 selected by using muon number

$E_1 < E_0 < E_2$ ⇒ $N_{\mu,1} < N_\mu < N_{\mu,2}$

Shower development stage (age) selected by using shower size

$N_{e,1} < N_e < N_{e,2}$

Frequency Attenuation: Constant N_e-N_μ cuts

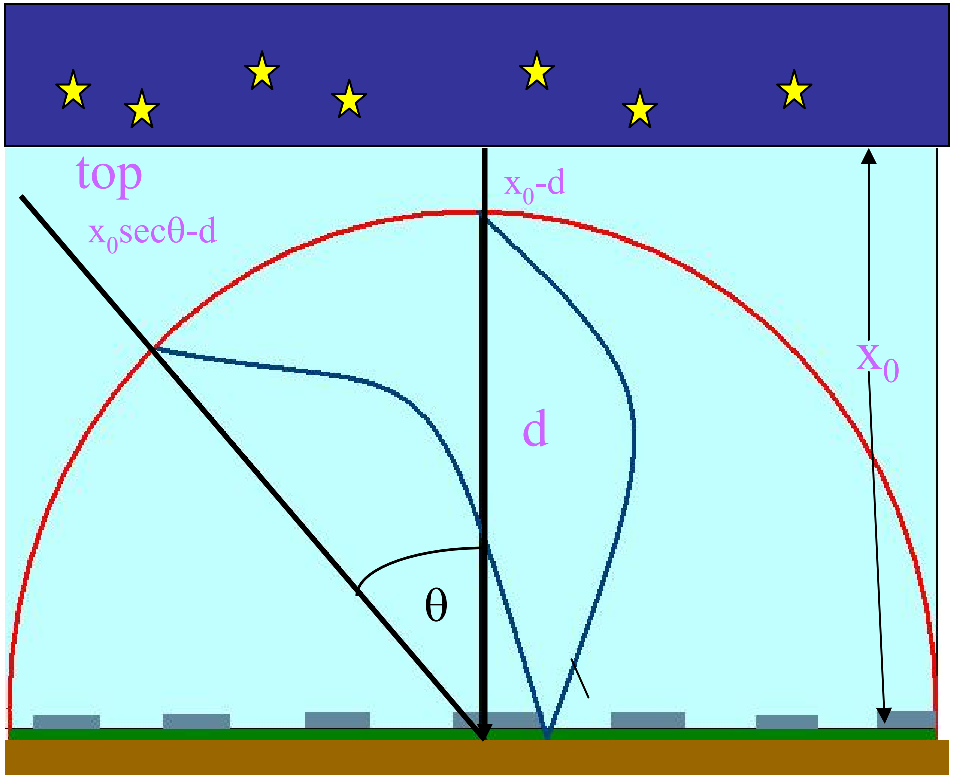

Primary Energy E_0 selected by using muon number

$E_1 < E_0 < E_2 \Rightarrow N_{\mu,1} < N_\mu < N_{\mu,2}$

Shower development stage (age) selected by using shower size

$N_{e,1} < N_e < N_{e,2}$

$$\Phi(\theta) = \Phi_0 \exp[-(x_0\sec\theta - d)/\lambda_{p\text{-}air}]$$

$$\Phi(\theta)/\Phi(0) = \exp[-(x_0\sec\theta - 1)/\lambda_{p\text{-}air}]$$

PRL 50 (1983) 2058
PRL 70 (1993) 2058

Fluctuations: *k* parameter

The observed absorption length is affected by fluctuations in the longitudinal development of cascades and in the detector response. The *k* parameter is obtained from simulation and accounts for all fluctuations:

$$k = \lambda_{sim}^{obs} \Big/ \lambda_{sim}^{p-air}$$

$$\lambda_{p\text{-air}}^{\exp} = \lambda_{obs}^{\exp} \Big/ k$$

$$\sigma_{p\text{-}air}^{inel} = k \cdot (14.5) / N \cdot \lambda_{obs} = 2.411 \cdot 10^{4} / \lambda_{p\text{-air}} \quad [mb]$$

EAS @ Max Development

$$R(\vartheta_1, \vartheta_2) = \frac{f(N_\mu, N_e, \vartheta_1)}{f(N_\mu, N_e, \vartheta_2)} = \exp\left[-\frac{X_v}{\Lambda_{obs}}(\sec\vartheta_1 - \sec\vartheta_2)\right]$$

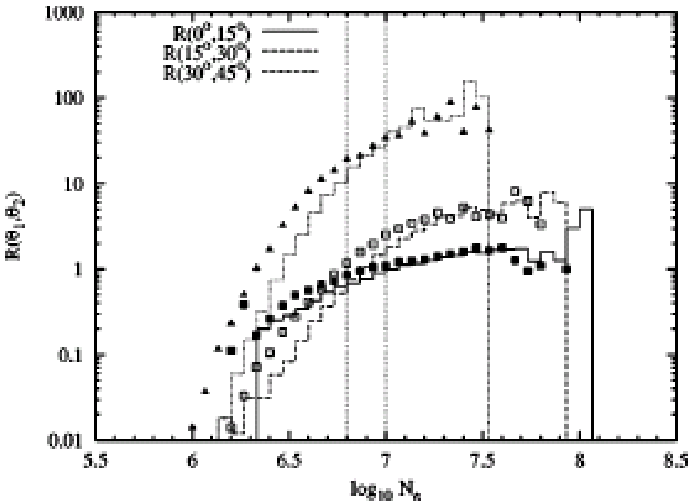

FIG. 5. Ratios of number of proton-initiated showers having between $10^{5.25}$ and $10^{5.45}$ muons and electron size N_e at 920 g/cm^2 as a function of N_e. Histograms correspond to showers simulated using SIBYLL 2.1, and points to showers simulated with QGSJET98.

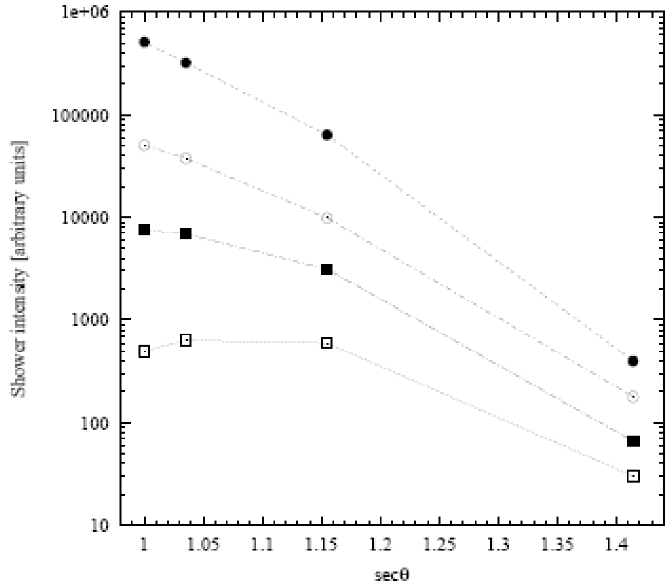

FIG. 6: Zenith angle dependence of the intensity of proton-induced showers having constant $\log_{10} N_\mu = 5.25 - 5.45$ and constant $\log_{10} N_e$ for different values of $\log_{10} N_e$. Empty squares $\log_{10} N_e = 6.8-7.0$, filled squares $\log_{10} N_e = 7.0-7.2$, empty circles $\log_{10} N_e = 7.2-7.4$ and filled circles $\log_{10} N_e = 7.4-7.6$. Showers were simulated with SIBYLL 2.1. The points are joined by straight lines to guide the eye. To avoid overlapping, the results for different N_e bins were multiplied by different arbitrary factors.

J.Alvarez-Muñiz et al., Phys. Rev D **66**, 123004

EAS @ Max Development

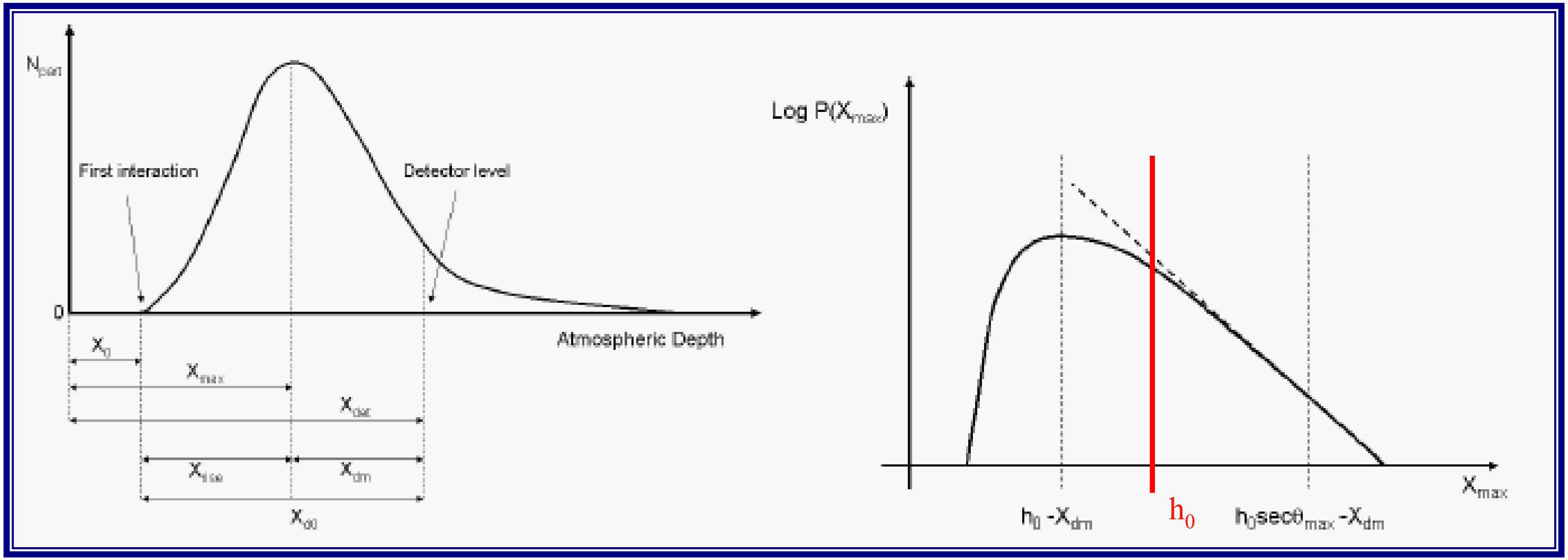

Fluctuation are lower if showers at maximum development are selected

This technique connot be applied by all ground based array experiments.

Once the primary CR energy (i.e. X_{max}), observation level (h_0) and angular range are defined, also the part of the X_{max} distribution that can be used is fixed.

EAS-TOP 1989-2000

Campo Imperatore

2000 m a.s.l. 820 g·cm^{-2}

10^{14} <E0 <10^{16}

- Hadrons
- E.M.
- Low Energy μ (E_μ > 1 GeV)
- Atmospheric Čerenkov Imaging
- H.E. μ (E > 1.3 TeV) (MACRO & LVD)

EAS-TOP *p*-air cross section at √s ≈ 2 TeV

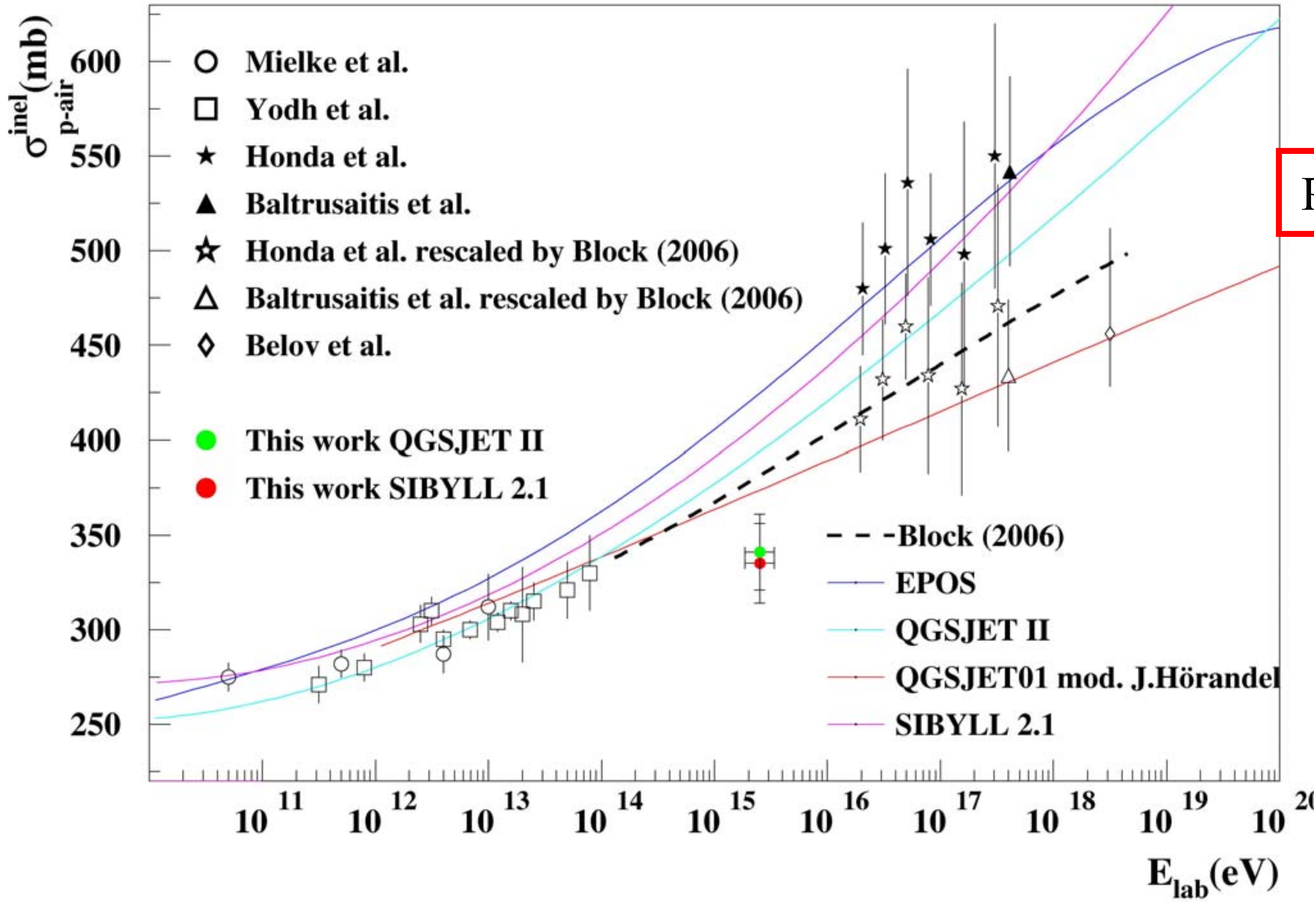

PRD 72 (2009) 032004

High energy hadronic interaction model	λ^{sim}_{int} [g/cm^2]	λ^{sim}_{obs} [g/cm^2]	k	λ^{exp}_{obs} [g/cm^2]	λ^{exp}_{int} [g/cm^2]	$\sigma^{inel}_{p\text{-}air}$ [mb]
SIBYLL 2.1	59.4 ± 0.1	69.9 ± 1.4	1.18 ± 0.02	84.7 ± 5.0	71.8 ± 4.5	336 ± 21
QGSJET II	60.3 ± 0.1	68.5 ± 1.4	1.14 ± 0.02	80.2 ± 4.3	70.7 ± 4.2	341 ± 20

Heavier Primaries

Helium QGSJET II

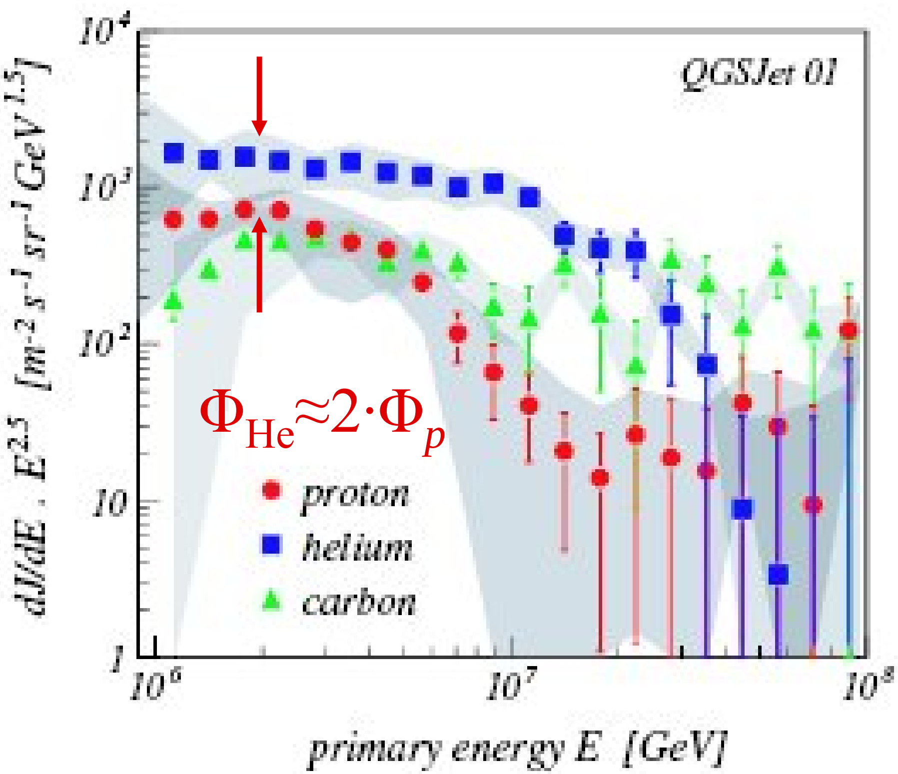

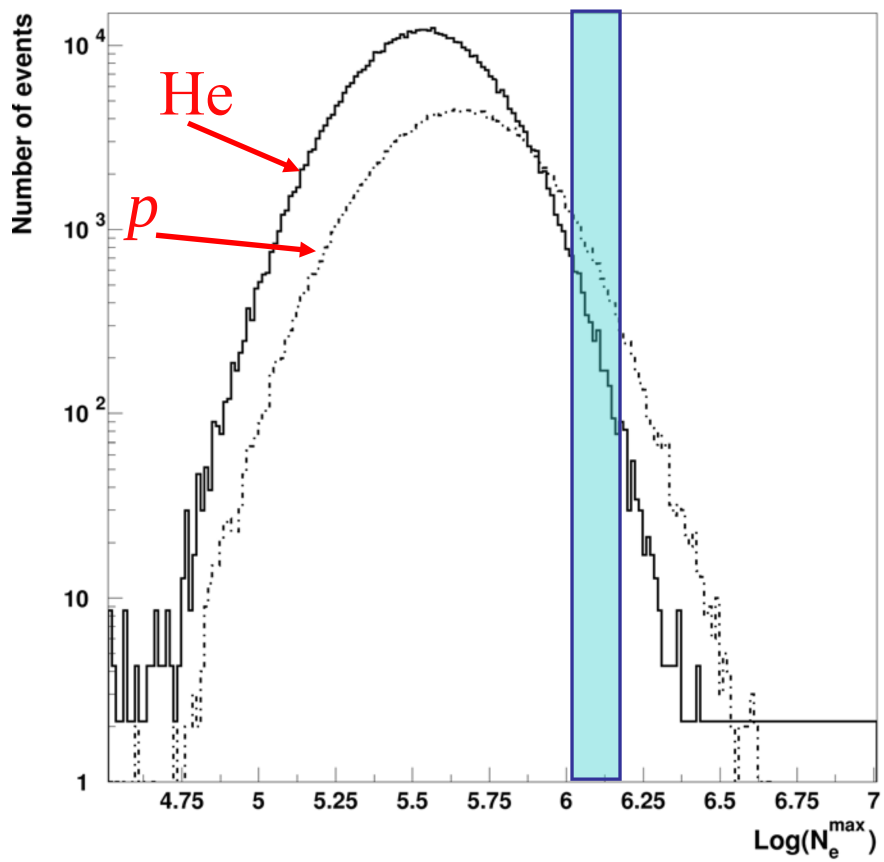

systematic uncertainty: σ_{sys}(He)= -29 mb

Systematic Uncertainties

In order to determine the systematic uncertainties due to the analysis procedure (e.g. HE interaction model), the cross section is reconstructed with a model that differs from the one used to produce the simulated datasets

Experiment	SIBYLL 2.1 $\sigma_{p\text{-air}}^{\text{inel}} = 406 \pm 1$ mb		QGSJET II $\sigma_{p\text{-air}}^{\text{inel}} = 400 \pm 1$ mb		QGSJET II$_{\text{HDPM}}$ $\sigma_{p\text{-air}}^{\text{inel}} = 367 \pm 1$ mb	
Analysis	$\sigma_{p\text{-air}}^{\text{inel}}$ [mb]	$\Delta\sigma_{p\text{-air}}^{\text{inel}}$ [mb]	$\sigma_{p\text{-air}}^{\text{inel}}$ [mb]	$\Delta\sigma_{p\text{-air}}^{\text{inel}})$ [mb]	$\sigma_{p\text{-air}}^{\text{inel}}$ [mb]	$\Delta\sigma_{p\text{-air}}^{\text{inel}}$ [mb]
SIBYLL 2.1	...	...	419 ± 12	$+19 \pm 12$	372 ± 13	$+5 \pm 13$
QGSJET II	393 ± 11	-13 ± 11	...	...	361 ± 12	-6 ± 12

Systematic Uncertainties

In order to determine the systematic uncertainties due to the analysis procedure (e.g. HE interaction model), the cross section is reconstructed with a model that differs from the one used to produce the simulated datasets

Experiment	SIBYLL 2.1 $\sigma^{\rm inel}_{p\text{-air}} = 406 \pm 1$ mb		QGSJET II $\sigma^{\rm inel}_{p\text{-air}} = 400 \pm 1$ mb		QGSJET $\rm II_{HDPM}$ $\sigma^{\rm inel}_{p\text{-air}} = 367 \pm 1$ mb	
Analysis	$\sigma^{\rm inel}_{p\text{-air}}$ [mb]	$\Delta\sigma^{\rm inel}_{p\text{-air}}$ [mb]	$\sigma^{\rm inel}_{p\text{-air}}$ [mb]	$\Delta\sigma^{\rm inel}_{p\text{-air}})$ [mb]	$\sigma^{\rm inel}_{p\text{-air}}$ [mb]	$\Delta\sigma^{\rm inel}_{p\text{-air}}$ [mb]
SIBYLL 2.1	...	...	419 ± 12	$+19 \pm 12$	372 ± 13	$+5 \pm 13$
QGSJET II	393 ± 11	-13 ± 11	...	...	361 ± 12	-6 ± 12

Systematic Uncertainties

In order to determine the systematic uncertainties due to the analysis procedure (e.g. HE interaction model), the cross section is reconstructed with a model that differs from the one used to produce the simulated datasets

Experiment	SIBYLL 2.1		QGSJET II		QGSJET II$_{HDPM}$	
	$\sigma^{inel}_{p\text{-air}} = 406 \pm 1$ mb		$\sigma^{inel}_{p\text{-air}} = 400 \pm 1$ mb		$\sigma^{inel}_{p\text{-air}} = 367 \pm 1$ mb	
Analysis	$\sigma^{inel}_{p\text{-air}}$ [mb]	$\Delta\sigma^{inel}_{p\text{-air}}$ [mb]	$\sigma^{inel}_{p\text{-air}}$ [mb]	$\Delta\sigma^{inel}_{p\text{-air}}$) [mb]	$\sigma^{inel}_{p\text{-air}}$ [mb]	$\Delta\sigma^{inel}_{p\text{-air}}$ [mb]
SIBYLL 2.1	...	...	419 ± 12	$+19 \pm 12$	372 ± 13	$+5 \pm 13$
QGSJET II	393 ± 11	-13 ± 11	...	...	361 ± 12	-6 ± 12

$$\sigma_{syst} = 19 \text{ mb} \ \ (99\% \text{ C.L.})$$

Systematic Uncertainties

In order to determine the systematic uncertainties due to the analysis procedure (e.g. HE interaction model), the cross section is reconstructed with a model that differs from the one used to produce the simulated datasets

Experiment	SIBYLL 2.1		QGSJET II		QGSJET II$_{HDPM}$	
	$\sigma^{inel}_{p\text{-air}} = 406 \pm 1$ mb		$\sigma^{inel}_{p\text{-air}} = 400 \pm 1$ mb		$\sigma^{inel}_{p\text{-air}} = 367 \pm 1$ mb	
Analysis	$\sigma^{inel}_{p\text{-air}}$ [mb]	$\Delta\sigma^{inel}_{p\text{-air}}$ [mb]	$\sigma^{inel}_{p\text{-air}}$ [mb]	$\Delta\sigma^{inel}_{p\text{-air}}$) [mb]	$\sigma^{inel}_{p\text{-air}}$ [mb]	$\Delta\sigma^{inel}_{p\text{-air}}$ [mb]
SIBYLL 2.1	...	...	419 ± 12	$+19 \pm 12$	372 ± 13	$+5 \pm 13$
QGSJET II	393 ± 11	-13 ± 11	...	...	361 ± 12	-6 ± 12

$\sigma_{syst} = 19$ mb (99% C.L.)

Systematic Uncertainties

In order to determine the systematic uncertainties due to the analysis procedure (e.g. HE interaction model), the cross section is reconstructed with a model that differs from the one used to produce the simulated datasets

Experiment	SIBYLL 2.1 $\sigma^{inel}_{p\text{-air}} = 406 \pm 1$ mb		QGSJET II $\sigma^{inel}_{p\text{-air}} = 400 \pm 1$ mb		QGSJET II$_{HDPM}$ $\sigma^{inel}_{p\text{-air}} = 367 \pm 1$ mb	
Analysis	$\sigma^{inel}_{p\text{-air}}$ [mb]	$\Delta\sigma^{inel}_{p\text{-air}}$ [mb]	$\sigma^{inel}_{p\text{-air}}$ [mb]	$\Delta\sigma^{inel}_{p\text{-air}}$) [mb]	$\sigma^{inel}_{p\text{-air}}$ [mb]	$\Delta\sigma^{inel}_{p\text{-air}}$ [mb]
SIBYLL 2.1	...	...	419 ± 12	$+19 \pm 12$	372 ± 13	$+5 \pm 13$
QGSJET II	393 ± 11	-13 ± 11	...	...	361 ± 12	-6 ± 12

$\sigma_{syst} = 19$ mb (99% C.L.)

EAS-TOP *p*-air cross section at $\sqrt{s} \approx 2$ TeV

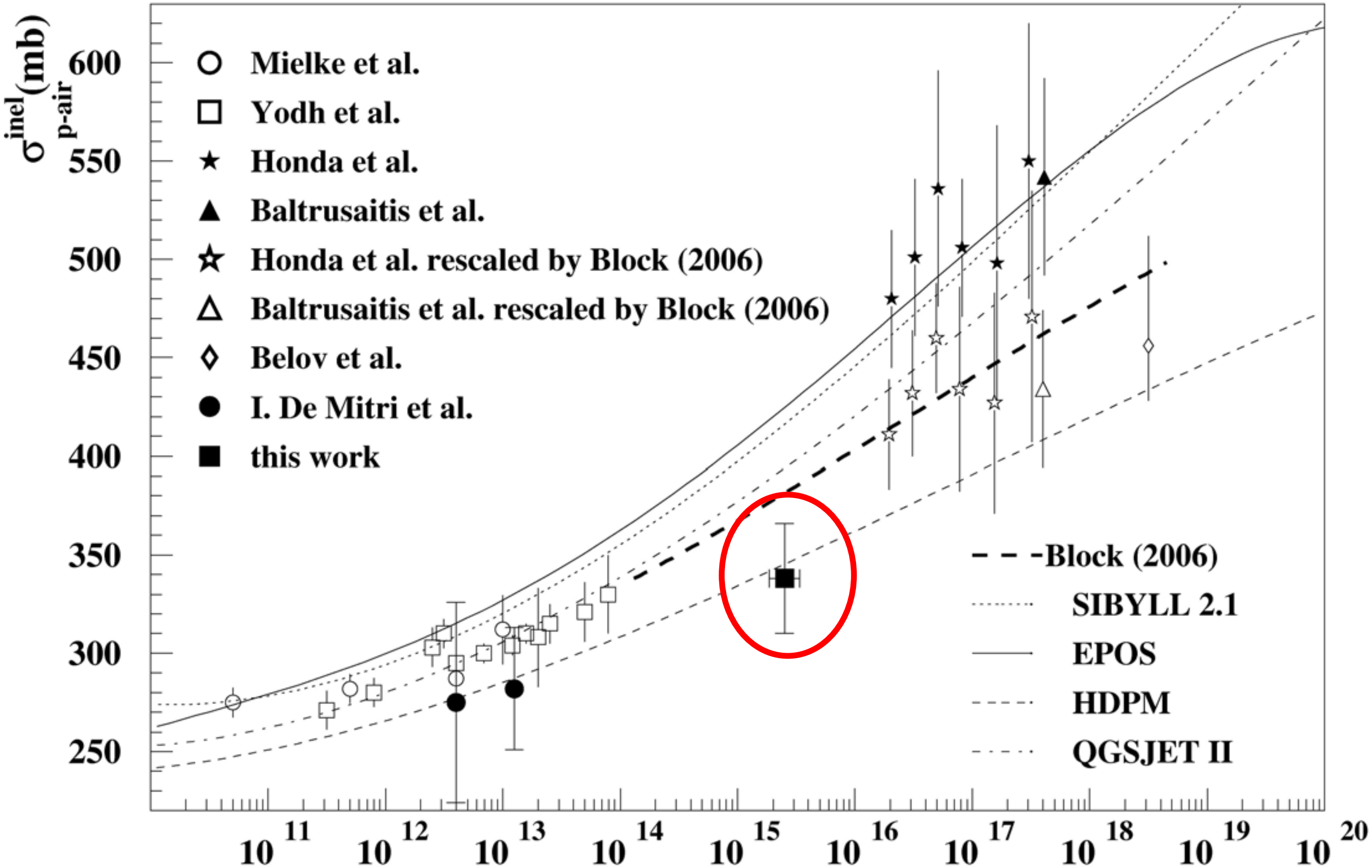

$$\sigma^{inel}_{p\text{-air}} = 338 \pm 21_{stat} \pm 19_{syst} - 29_{syst(He)} \text{ mb}$$

PRD 72 (2009) 032004

ARGO-YBJ collaboration

High Altitude Cosmic Ray Laboratory at YangBaJing

Longitude 90° 31’ 50” East
Latitude 30° 06’ 38” North

4300 m above the sea level
$E_0 \approx 10^{12}$ eV ÷ 10^{15}GeV
610 g/cm^2

Astrophysical
Radiation
Ground-based
Observatory @
YangBaJing

ARGO-YBJ *p*-air cross section

$\sqrt{s}$ = 70 GeV ÷ 500 GeV

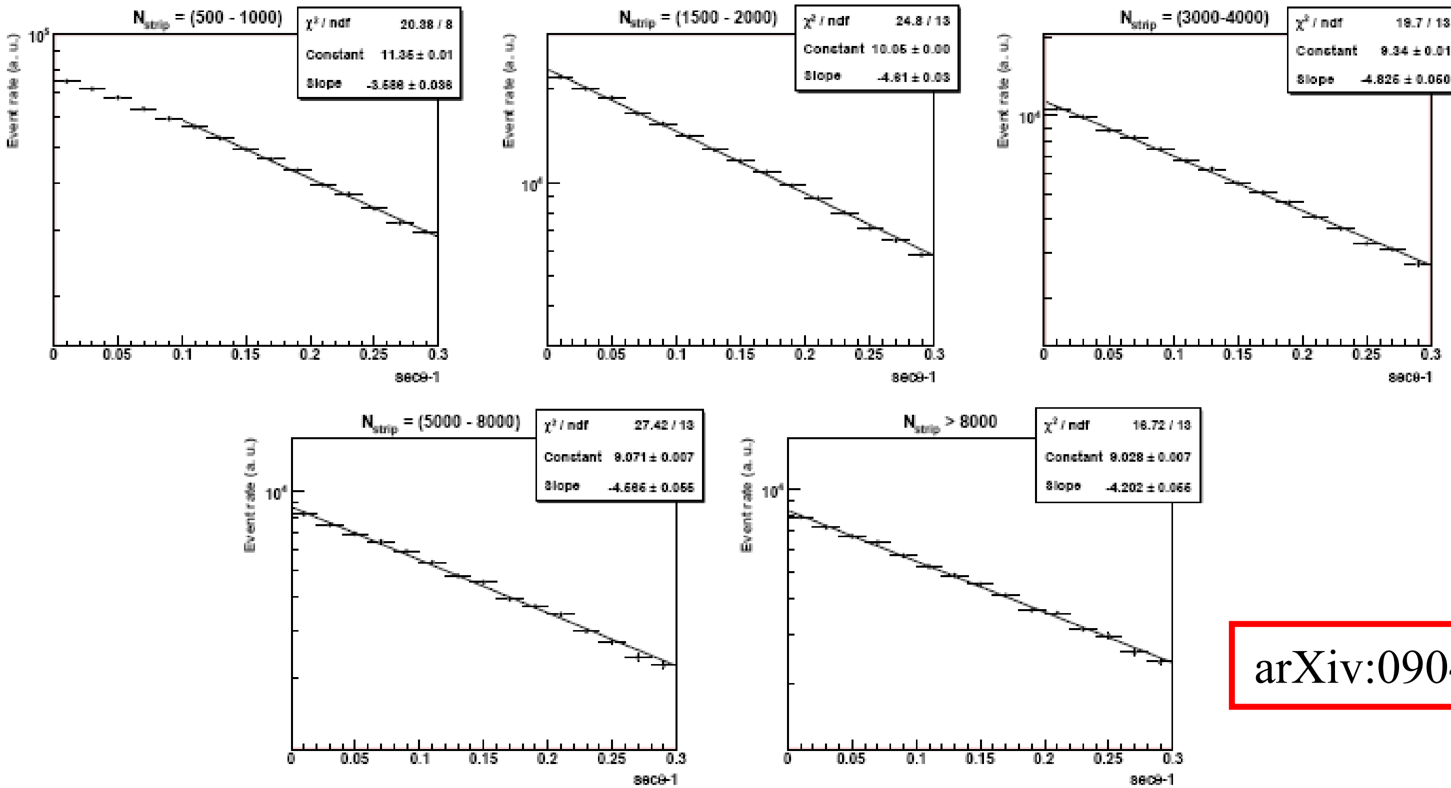

arXiv:0904.4198

ΔN_{strip}	$\mathrm{Log}(E/\mathrm{eV})$	$k_{QGSJET-I}$	$k_{QGSJET-II.03}$	$k_{SIBYLL-2.1}$	k
500 ÷ 1000	12.6 ± 0.3	$1.98 \pm 0.06 \pm 0.05$	$1.84 \pm 0.14 \pm 0.05$	$1.87 \pm 0.08 \pm 0.04$	$1.93 \pm 0.05 \pm 0.06$
1500 ÷ 2000	13.0 ± 0.2	$1.59 \pm 0.03 \pm 0.04$	$1.75 \pm 0.12 \pm 0.04$	$1.76 \pm 0.06 \pm 0.04$	$1.63 \pm 0.03 \pm 0.08$
3000 ÷ 4000	13.3 ± 0.2	$1.69 \pm 0.05 \pm 0.03$	$1.63 \pm 0.13 \pm 0.03$	$1.72 \pm 0.05 \pm 0.03$	$1.70 \pm 0.03 \pm 0.04$
5000 ÷ 8000	13.6 ± 0.2	$1.74 \pm 0.05 \pm 0.03$	$1.97 \pm 0.17 \pm 0.04$	$1.91 \pm 0.05 \pm 0.03$	$1.84 \pm 0.03 \pm 0.10$
> 8000	13.9 ± 0.3	$2.04 \pm 0.06 \pm 0.05$	$2.23 \pm 0.19 \pm 0.05$	$2.01 \pm 0.05 \pm 0.05$	$2.03 \pm 0.04 \pm 0.10$

Heavy primaries contribution

Hoerandel AP 19 (2003) 193 taken as reference.

JACEE and RUNJOB for the evaluation of systematic error

$$\frac{dN}{dE} = \Phi(E) = \Phi_Z^0 \cdot \left(\frac{E}{TeV}\right)^{-\gamma_Z}$$

198 J.R. Hörandel / Astroparticle Physics 19 (2003) 193–220

Table 1
Absolute flux Φ_Z^0 ((m^2 sr s TeV)$^{-1}$) at $E_0 = 1$ TeV/nucleus and spectral index γ_Z of cosmic-ray elements

Z		Φ_Z^0	$-\gamma_Z$	Z		Φ_Z^0
1[a]	H	8.73×10^{-2}	2.71	47[c]	Ag	4.54
2[a]	He	5.71×10^{-2}	2.64	48[c]	Cd	6.30
3[b]	Li	2.08×10^{-3}	2.54	49[c]	In	1.61
4[b]	Be	4.74×10^{-4}	2.75	50[c]	Sn	7.15
5[b]	B	8.95×10^{-4}	2.95	51[c]	Sb	2.03
6[b]	C	1.06×10^{-2}	2.66	52[c]	Te	9.10
7[b]	N	2.35×10^{-3}	2.72	53[c]	I	1.34
8[b]	O	1.57×10^{-2}	2.68	54[c]	Xe	5.74
9[b]	F	3.28×10^{-4}	2.69	55[c]	Cs	2.79
10[b]	Ne	4.60×10^{-3}	2.64	56[c]	Ba	1.23

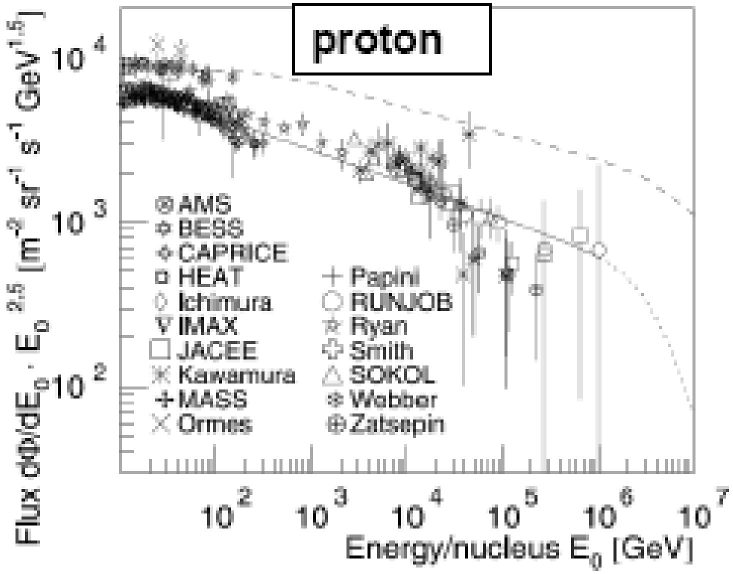

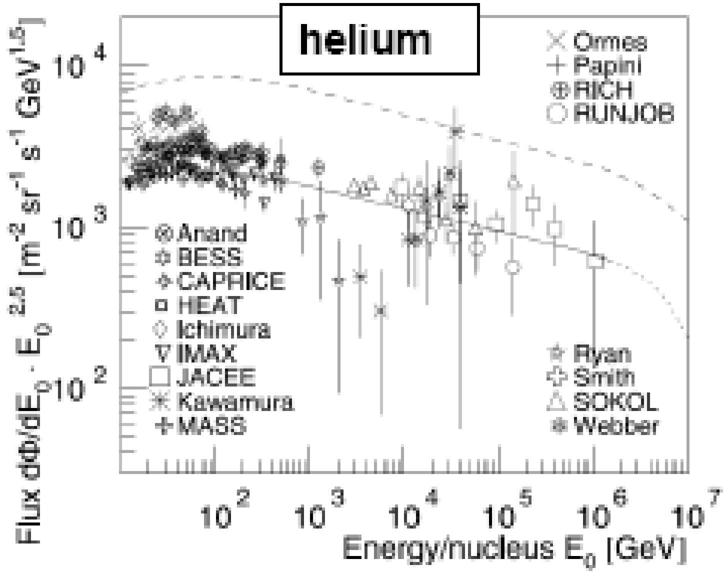

ARGO-YBJ *p*-air cross section
$\sqrt{s}$ = 70 GeV ÷ 500 GeV

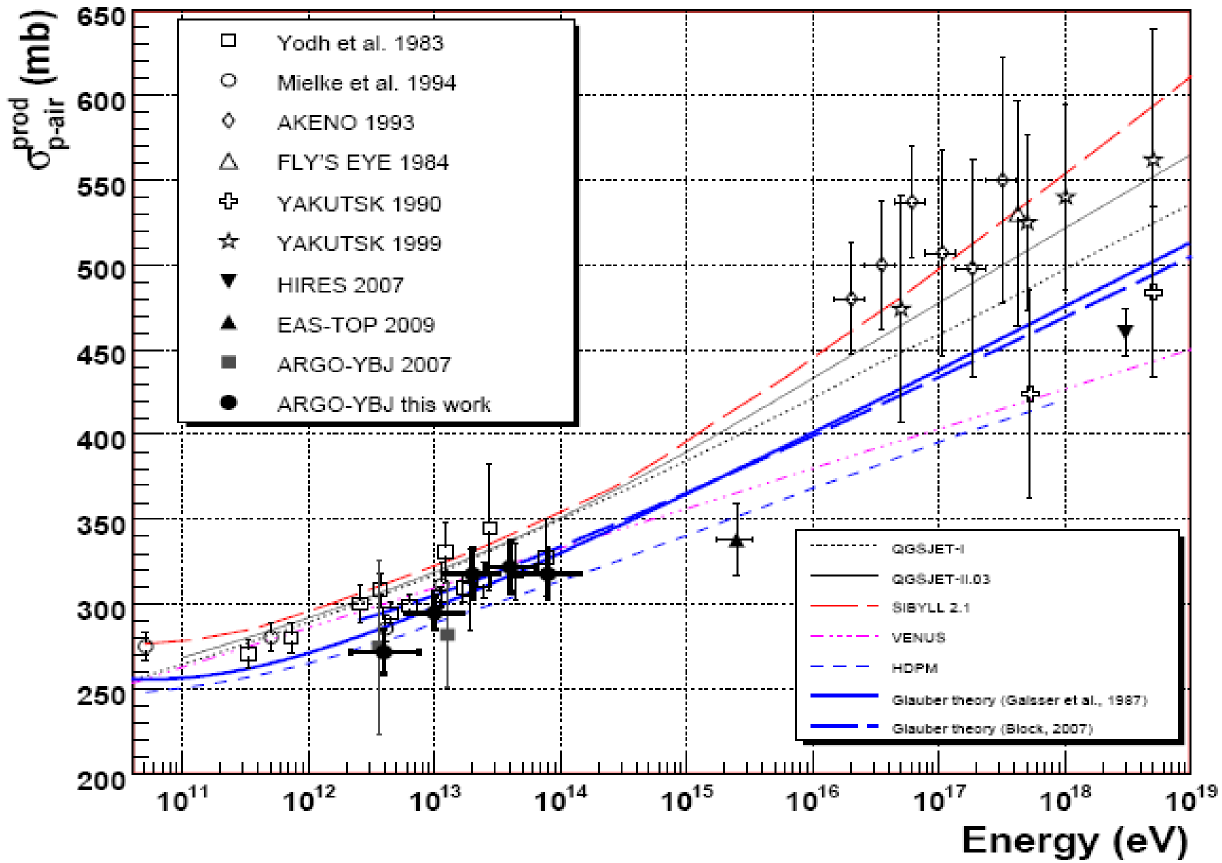

arXiv:0904.4198

ΔN_{strip}	η	σ_{p-air} (mb)	σ_{p-p} (mb)
500 ÷ 1000	$1.00 \pm 0.04 \pm 0.01$	$272 \pm 13 \pm 9$	$43 \pm 3 \pm 5$
1500 ÷ 2000	$1.00 \pm 0.03 \pm 0.01$	$295 \pm 10 \pm 14$	$48 \pm 3 \pm 6$
3000 ÷ 4000	$0.99 \pm 0.04 \pm 0.01$	$318 \pm 15 \pm 8$	$54 \pm 4 \pm 6$
5000 ÷ 8000	$0.98 \pm 0.04 \pm 0.03$	$322 \pm 15 \pm 20$	$56 \pm 4 \pm 7$
> 8000	$0.95 \pm 0.04 \pm 0.04$	$318 \pm 15 \pm 21$	$54 \pm 4 \pm 8$

HiRes *p*-air cross section at $\sqrt{s} \approx 80$ TeV

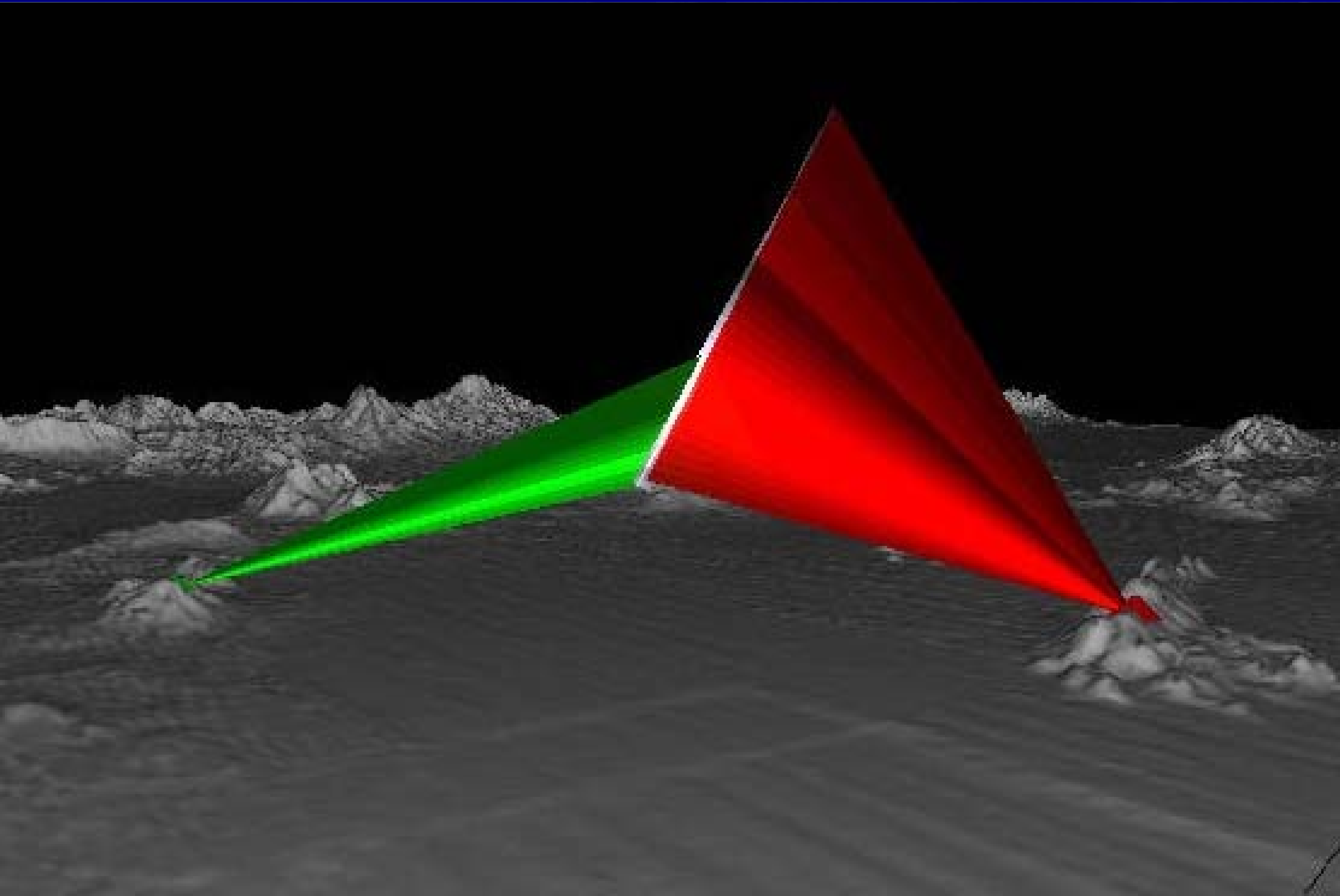

HiRes *p*-air cross section at $\sqrt{s} \approx 70$ TeV

Point of first interaction distribution. Exponential index reflects inelastic Cross-section

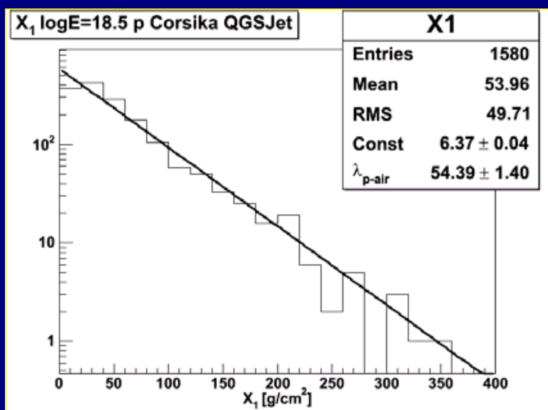

$$f_{\rm int} = e^{-\frac{x_1}{\lambda_{p-Air}}};$$

$$\lambda_{p-Air} = \frac{1}{\tilde{n}\,\sigma^{inel}_{p-air}};$$

$\otimes$

Atmospheric part of air shower fluctuations

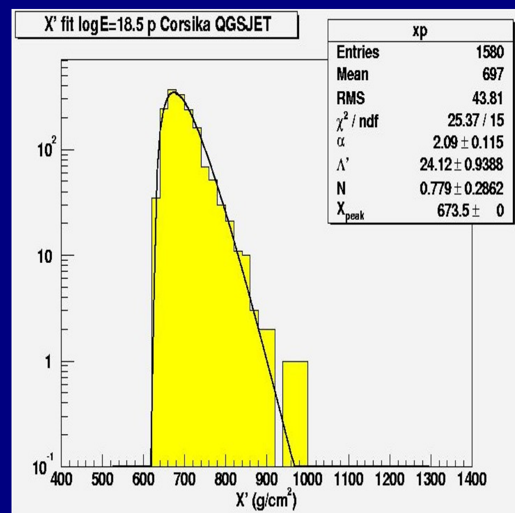

$$X' = X_{\max} - X_1$$

$$f_{fluct} = \left[\frac{x_{\max} - x_{peak} - x_1 + \Lambda'\alpha}{e}\right]^{\alpha} e^{-\frac{x_{\max} - x_1 - x_{peak}}{\Lambda'}}$$

$$f_{fluct}(x_{peak}(E), \Lambda'(E), \alpha(E)) \Rightarrow f_{fluct}(E)$$

=

X_{max} distribution

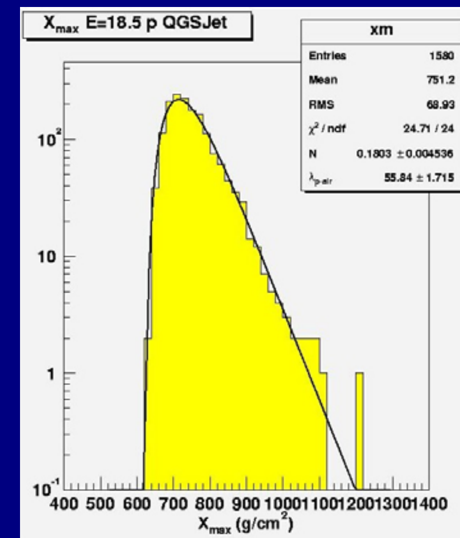

$$P_m(x_m) = \left(e^{-\frac{x_1}{\lambda_{p-air}}}\right) \otimes \left(\left[\frac{x_{\max} - x_{peak} - x_1 + \Lambda'\alpha}{e}\right]^{\alpha} e^{-\frac{x_{\max} - x_1 - x_{peak}}{\Lambda'}}\right) \Rightarrow N \int_0^{x_m - x_{peak} + \Lambda'\alpha} e^{\frac{-x_1}{\lambda_{p-Air}}} \left[\frac{x_{\max} - x_{peak} - x_1 + \Lambda'\alpha}{e}\right]^{\alpha} e^{-\frac{x_{\max} - x_1 - x_{peak}}{\Lambda'}} dx_1;$$

HiRes *p*-air cross section at $\sqrt{s} \approx 70$ TeV

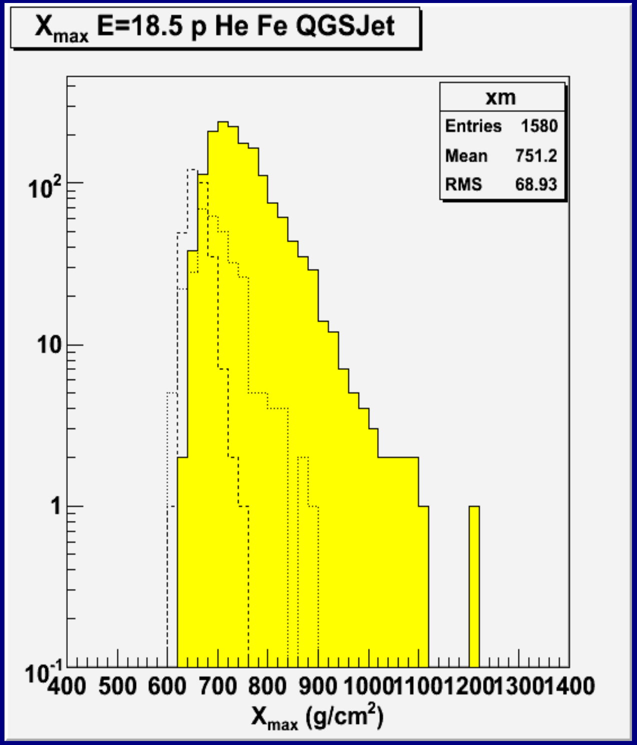

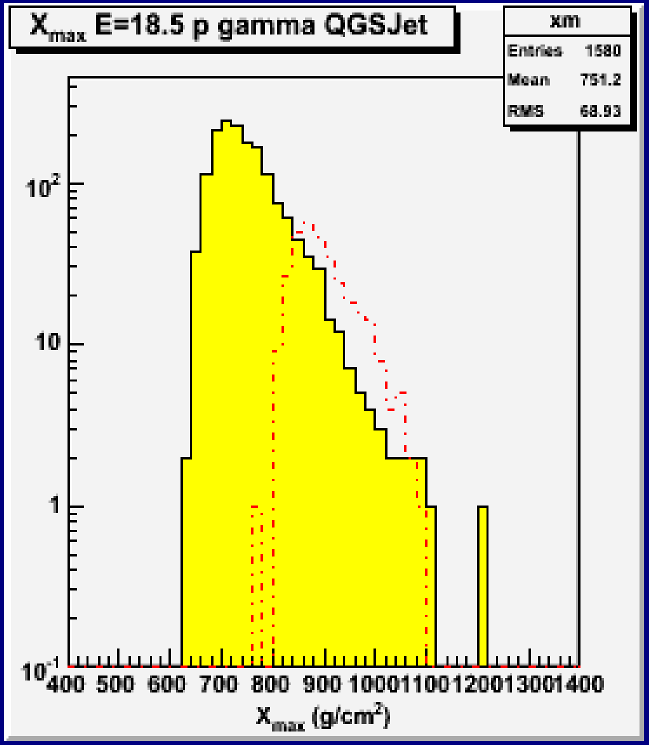

- Fe is cut off by using the deeper portion of the Xmax distribution;
- He and gamma has to be taken into account;

HiRes *p*-air cross section at $\sqrt{s} \approx 70$ TeV

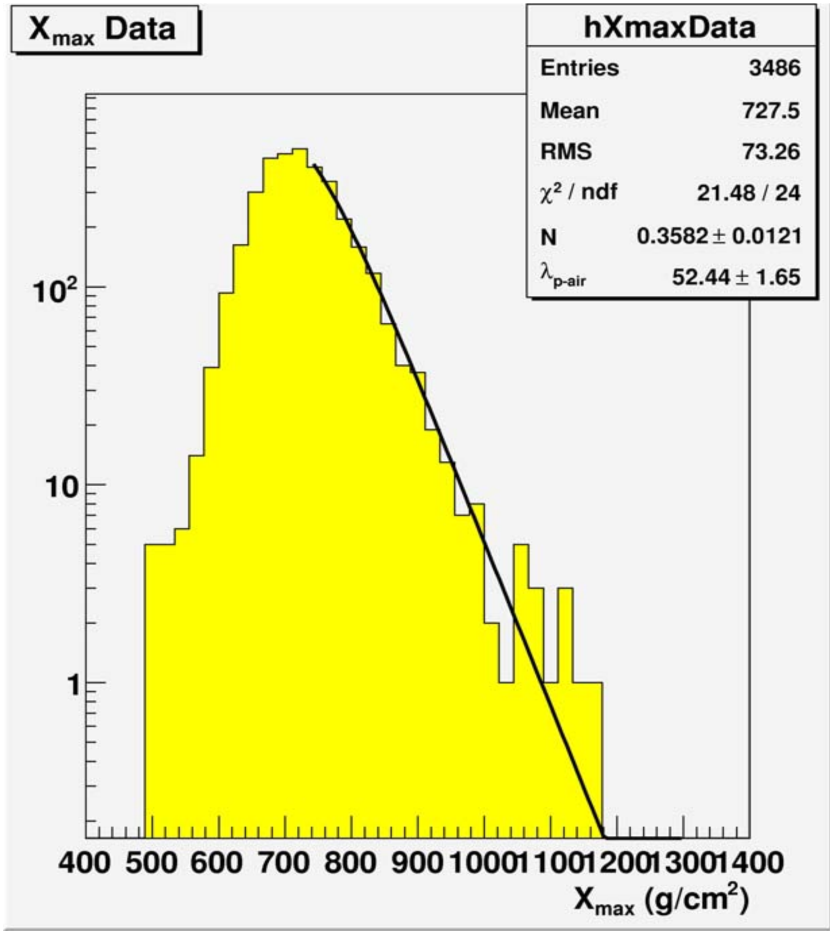

- Mean energy ~ $10^{18.5}$ eV;

Nuclear Physics B 151 (2006) 197

$$\sigma_{in}^{p-Air} = 460 \pm 14\,(stat) + 39(sys) - 26\,(sys)\ mb$$

EAS-TOP: *p*-air ⟷ *pp* at $\sqrt{s} \approx 2$ TeV

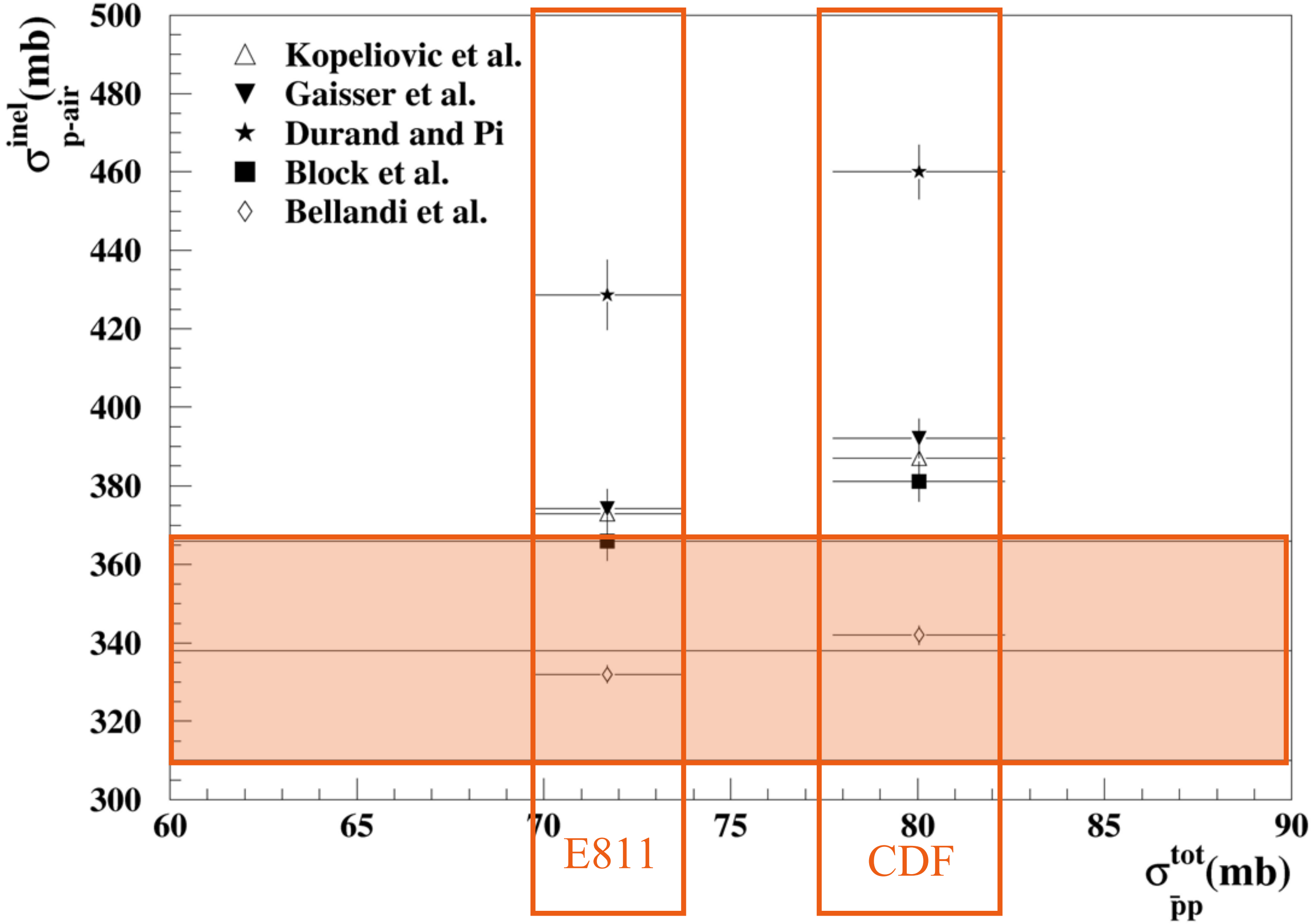

PRD 72 (2009) 032004

p-p total cross section

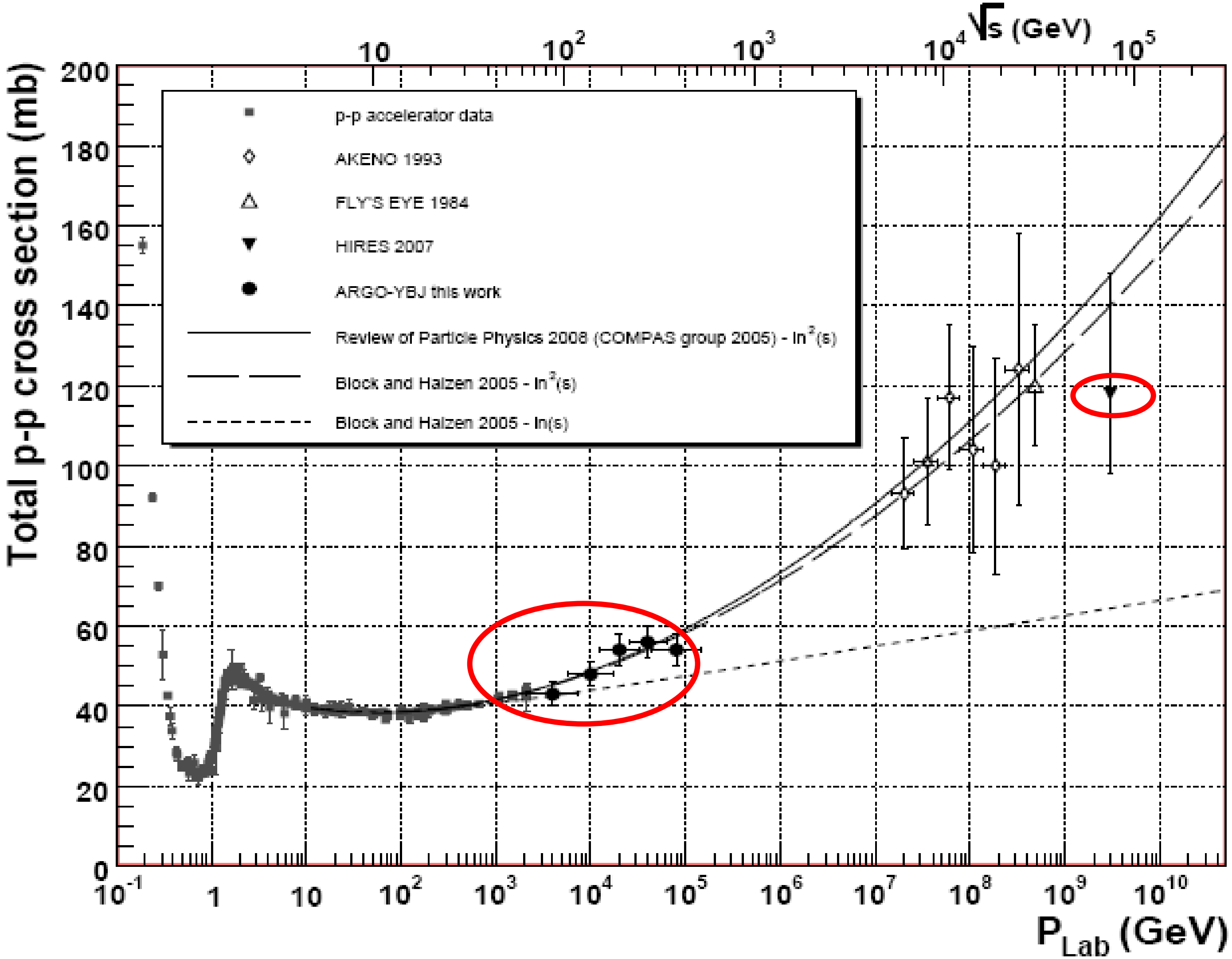

Conclusions

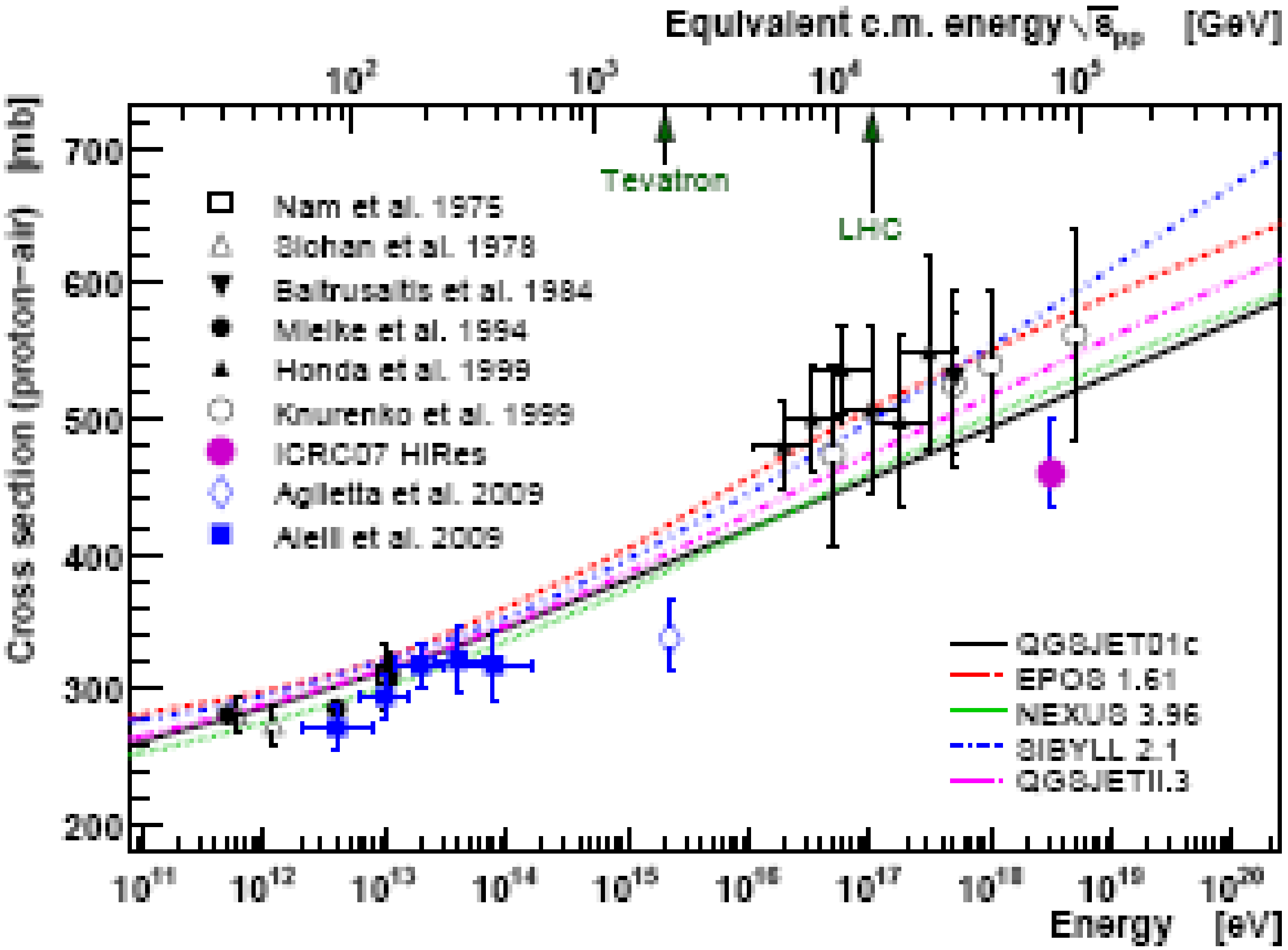

Conclusions

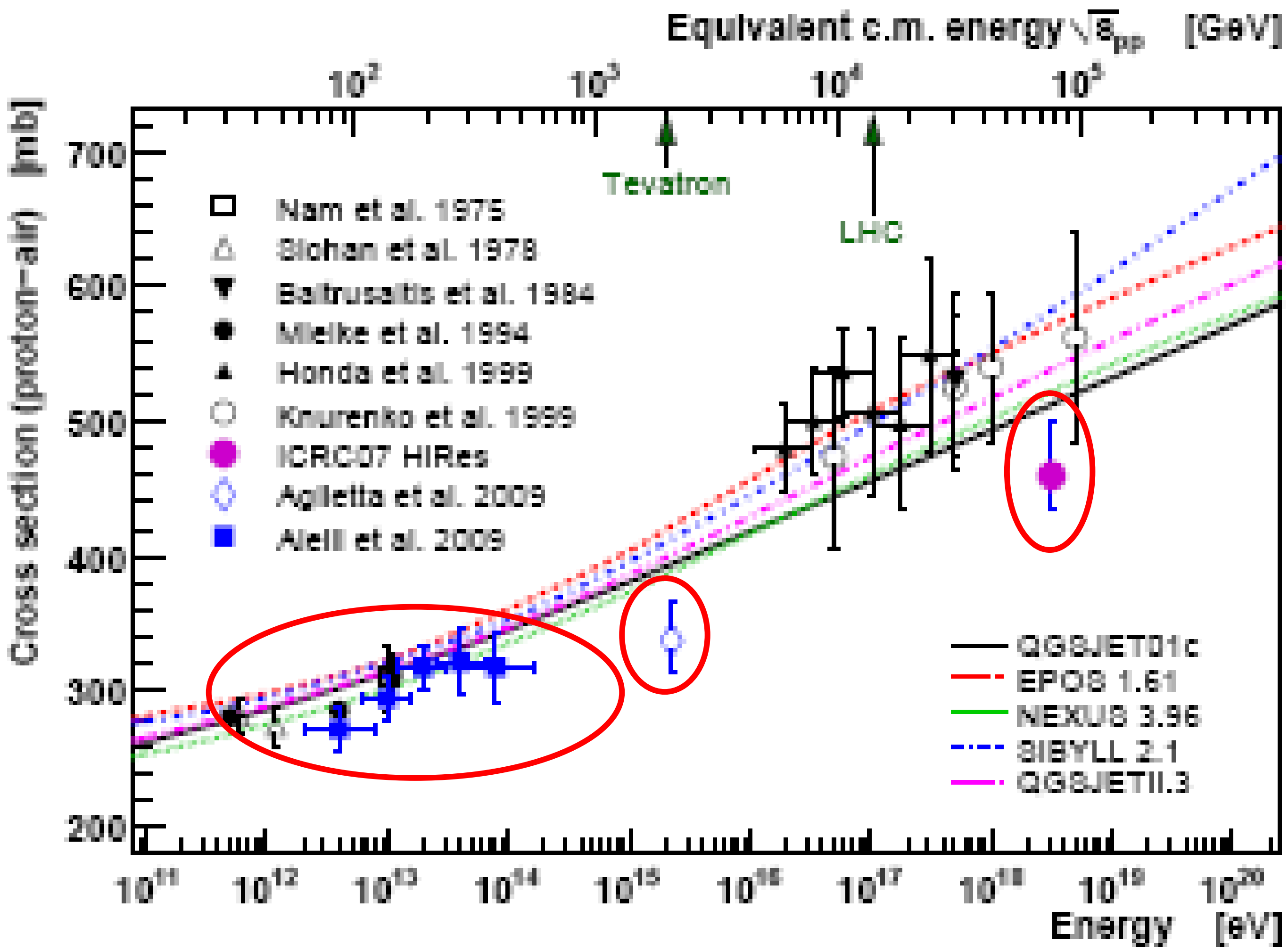

Conclusions

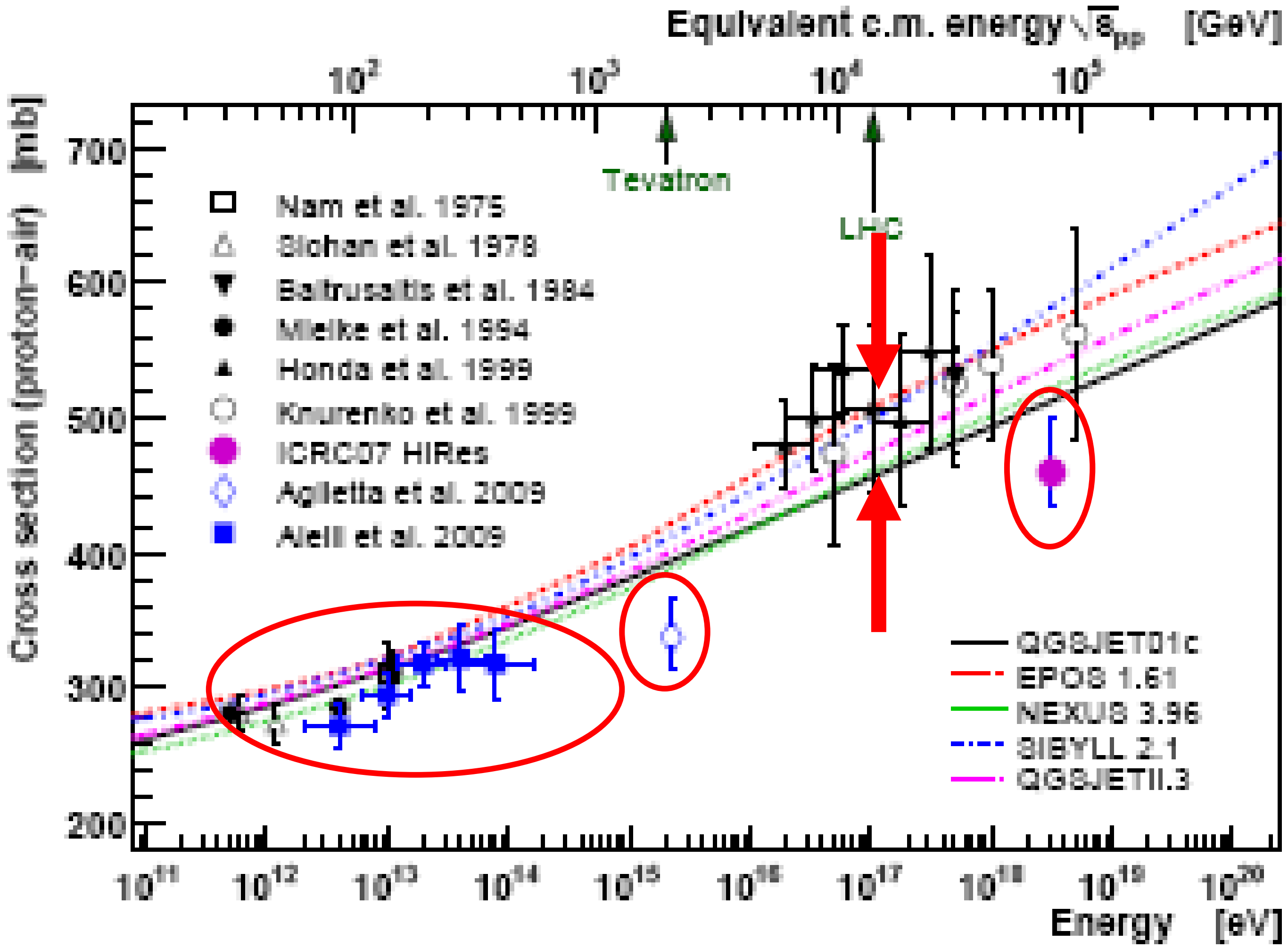

Conclusions